LASER INTERFEROMETER GRAVITATIONAL WAVE OBSERVATORY
- LIGO -
CALIFORNIA INSTITUTE OF TECHNOLOGY
MASSACHUSETTS INSTITUTE OF TECHNOLOGY

Document Type **LIGO-T990130-02-D** January, 1999

LIGO ASC Subsystem: Wavefront Sensing Telescopes

Nergis Mavalvala

Distribution of this draft:

ISC

This is an internal working note
of the LIGO Project.

California Institute of Technology
LIGO Project - MS 51-33
Pasadena CA 91125
Phone (818) 395-2129
Fax (818) 304-9834
E-mail: info@ligo.caltech.edu

Massachusetts Institute of Technology
LIGO Project - NW 17-161
Cambridge, MA 01239
Phone (617) 253-4824
Fax (617) 253-7014
E-mail: info@ligo.mit.edu

WWW: http://www.ligo.caltech.edu/

Introduction

The purpose of this document is to specify the design of the Guoy phase telescopes which are part of the wavefront sensing alignment scheme for the detector. The telescopes are used to address two constraints on the Gaussian beam at the detection plane: first, that the Guoy phase be optimized for maximum detection of the primary degree of freedom, and second, that the spot size be 'matched' to the size of the quadrant diode. The Guoy phase corresponding to maximum sensitivity to each degree of freedom is calculated using the Modal Model [1]. The optimal spot size for the EG&G YAG-444-4A quadrant photodiodes to be used in the wavefront sensors is about 3 mm (calculated below). In this document we determine the focal lengths and positions of lenses and the positions of the detectors that give this Guoy phase shift.

A schematic layout of the Interferometer Sensing and Control (ISC) interferometric sensors is shown in Figure 1. Only the interferometer sensors are shown, though the ISC tables will contain

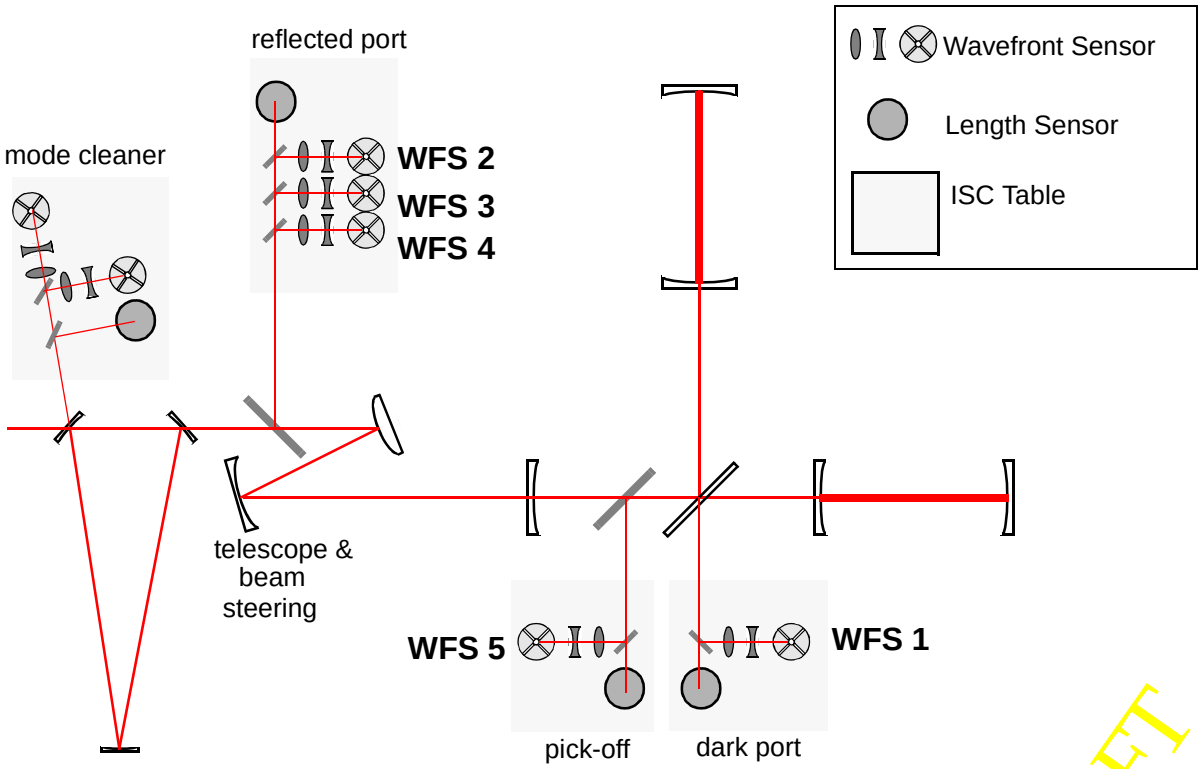

Figure 1: Functional layout of the ISC interferometric sensors. The 'pick-off' represents a beam from one of the ITM, or the BS, AR surfaces. The 'reflected port' is representative of a sample of the interferometer reflected light.

many other components. The Guoy phase telescope component locations must be compatible with the shared table space.

Alignment sensitivity matrix

The alignment sensitivity matrix is calculated in Ref. [2]. The results are summarized in Table 1.

Wavefront Sensor				Angular degree of freedom				
# (port)	f_{mod}	Φ_{RF}	Φ_{Guoy}	ΔETM	ΔITM	$\overline{ETM}$	$\overline{ITM}$	RM
WFS 1 (dark)	f_{res}	Q	90°	**-0.044**	**-0.02**	0	0	0
WFS 2 (refl)	f_{res}	I	145°	0	0	-2.0×10^{-3}	**0.026**	**-0.041**
WFS 2b (refl)	f_{res}	Q	145°	9.6×10^{-5}	$\mathbf{-5.8 \times 10^{-3}}$	0	4.6×10^{-4}	-7.0×10^{-4}
WFS 3 (refl)	f_{NR}	I	0°	0	0	-7.0×10^{-4}	-3.2×10^{-4}	$\mathbf{7.3 \times 10^{-3}}$
WFS 4 (refl	f_{NR}	I	90°	0	0	$\mathbf{-8.0 \times 10^{-3}}$	$\mathbf{-3.7 \times 10^{-3}}$	6.4×10^{-4}
WFS 5 (pick-off)	f_{res}	Q	145°	6.5×10^{-4}	**-0.039**	0	3.2×10^{-3}	-4.4×10^{-3}

Table 1: Matrix of misalignment error signals with the sensor locations and detection phases. The matrix elements for the 4 km interferometer (4k) are listed, but the matrix is nearly identical for the 2 km interferometer (2k), with only small differences in the amplitude of the error signals for the same RF and Guoy phases. Units are Watts per normalized angle ($\Theta_D = 9.6 \times 10^{-6}$ rad for the 4k and $\Theta_D = 10.9 \times 10^{-6}$ rad for the 2k).

The parameters used to calculate the alignment sensitivity matrix are listed in Tables 1 and 11 of Ref. [2]. There have been small changes in some of these parameters, e.g. mirror radii of curvature, but will have little influence on the calculation of the alignment matrix. Φ_{Guoy} listed in is the Guoy phase required *at the wavefront sensor* for optimal detection. Consequently, all the Guoy phase accumulated in propagating the beam from the interferometer beam waist to the wavefront sensor must be accounted for.

Design constraints

The following practical considerations have driven the design choices:

- The nearest accessible position to the reflection port is about 4 m away, so $z_1 \geq 4.0$ m.
- Separation between lenses must be large enough to accommodate other optics on the ISC tables, so $z_2 - z_1 \geq 0.25$ m.
- The total distance between the telescopes and the detector should not exceed 2.5 m, so $z_{det} - z_1 \leq 2.5$ m.

- The electro-optic shutter has a clear aperture of 8 mm so the spot size on it should not exceed 5 mm in diameter.
- The optimum spot size on the detector is determined by the size of the quadrant photodiodes [4]. The EG&G YAG 444-4 have an active area of 1 cm^2, which gives detector radius, $R = 5.64$ mm .The ratio of the spot size on the detector, w, to the detector radius, R, which ensures that less than 1% of the signal is lost due to the finite detector size is $w/R \leq 0.6$. This corresponds to $w \leq 3.4$ mm . **We use $w = 2.5$ mm** .
- We use commercial off-the-shelf lenses; their focal lengths must be accordingly chosen.

Lens selection

To minimize spherical aberrations, we use a plano-convex lens for lens 1 and a bi-concave lens for lens2. The CVI lenses we choose have good surface quality and figure, with a small error in the focal length. Specifically, for CVI lenses

- Surface quality: 10-5 scratch-dig (cf. 40-20 for same Newport lens)
- Surface figure: l/10 at 633 nm (cf. λ/4 to λ/2 at 546 nm for Newport)
- Focal length tolerance: ±0.5% (cf. ±2% for Newport)

The part numbers for the lenses used in the design of the Guoy phase telescopes (below) are:

CVI PLCX-25.4-515.1-C with f(1064 nm) = +1016.7 mm
CVI BICC-25.4-77.6-C with f(1064 nm) = –76.3 mm
CVI BICC-25.0-26.1-C with f(1064 nm) = –25.4 mm

As shown in Figure 1, there are three interferometer detection ports with an ISC photodetection table at each port. Since the beam characteristics and beam delivery optics at each port is different, it is necessary to address the Guoy phase telescope design at each port independently.

Antisymmetric port

i Telescope layout and definitions

WFS 1 in Table 1 is located at the antisymmetric port. A schematic of the layout for the antisymmetric port photodetection is shown in Figure 2. The beam passes through a beam

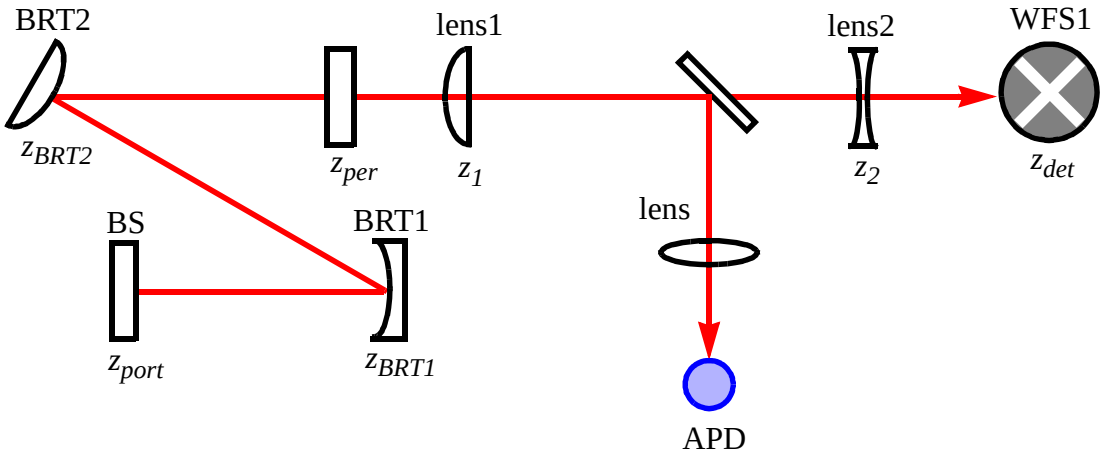

Figure 2: Schematic layout of the wavefront sensors at the antisymmetric. z_{port} is the location of the beamsplitter, which is also the antisymmetric port. From the BS, the beam travels through the beam reducing telescope (BRT) and arrives at the periscope on ISCT 3. We set $z = 0$ at the position of the beam waist of the beam returning from the BRT. z_{port} is the position of the BS; z_{BRTi} are the positions of the i-th BRT mirrors; z_{per} is the position of the periscope; z_1 is the position of the first lens, with focal length, f_1; z_2 is the position of the second lens, with focal length, f_2; and z_{det} is the position of the detector.

reducing telescope. For the purposes of the design, we propagate the arm cavity beam through the beam reducing telescope to determine the plane at which the BRT output beam has a waist. The waist position and size and the total Guoy phase accumulated from the interferometer beam waist to this plane are the inputs to the Guoy phase telescope optimization algorithm. Some parameters that are relevant to the calculation are listed in Table 2 [7], [8]. The beam propagated through the antisymmetric port BRT has an effective beam waist w_0 = 3.819 mm occurring 20.0489 m behind (i.e. towards the vacuum viewport) the periscope. The total Guoy phase shift accumulated to the periscope output is 20°.

The focal lengths and positions of the lenses and the position of the detector head for the antisymmetric port telescope is given in Table 3. The parameter Δz is distance by which the second lens position is moved to make the “far field” or “infinity adjustment” [9]. Negative (positive) values for Δz correspond to moving lens 2 closer to (farther from) lens 1. We note that

Optical train	Geometric parameters	Relative position[a] (m)
Arm cavity beam waist	$w_0 = 3.13$ cm	0
ITM	$R = 14200$ m $\Rightarrow f = -31556$ m	613.6
BRT1	$f = 1.5240$ m	4.461[b]
BRT2	$f = -0.1905$ m	1.3335
Vacuum viewport	flat	5.402
Periscope bottom mirror	flat	1.140

Table 2: The geometric parameters and positions of the optical elements between the arm cavity beam waist and the periscope on the antisymmetric port output table for the 2 km configuration

a. Position of the optical element relative to the previous element in the optical train, i.e. the spacing between adjacent optical elements.
b. Distance from beamsplitter to BRT lens 1. Here I assume that the ITM and BS are collocated.

WFS (Φ_{Guoy})	Ifo	f_1	z_1	f_2	z_2	z_{det}	Δz
WFS 1 (90°)	4k	+1016.7		–25.4			
WFS 1 (90°)	2k	+1016.7	330.0	–25.4	1324.4	1882.2	5.9

Table 3: The Guoy phase telescopes for the antisymmetric port wavefront sensors for the 4 km and 2 km configurations. All distances are in mm and are specified from $z = 0$ at the location of the bottom mirror of the periscope on ISCT3. Only the shaded boxes are revised in the present version of this document.

in order to keep the total length of the Guoy phase telescope from being too long, WFS 1 is a special case where we arrange the spot size on the detector head to be 2 mm rather than 2.5 mm.

The Gaussian beam propagation, along with Guoy phase shift along the telescope train is give in Figure 3 for the 2 km configuration.

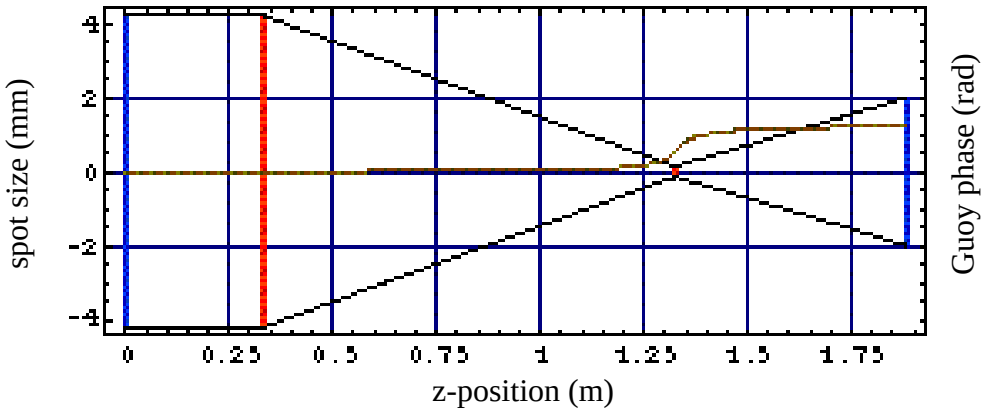

Figure 3: Gaussian beam profile for the 2 km configuration for the antisymmetric port sensor, WFS 1. The Guoy phase shift is shown as the gold curve and does not include the 20° already accumulated by propagation from the interferometer beam waist out to the periscope output (z = 0 in the above plot).

Reflection port

i Telescope layout and definitions

WFS 2, WFS 3 and WFS 4 in Table 1 are located at the reflection port. A schematic of the layout for the reflection port photodetection is shown in Figure 4. The beam returning from the recycling

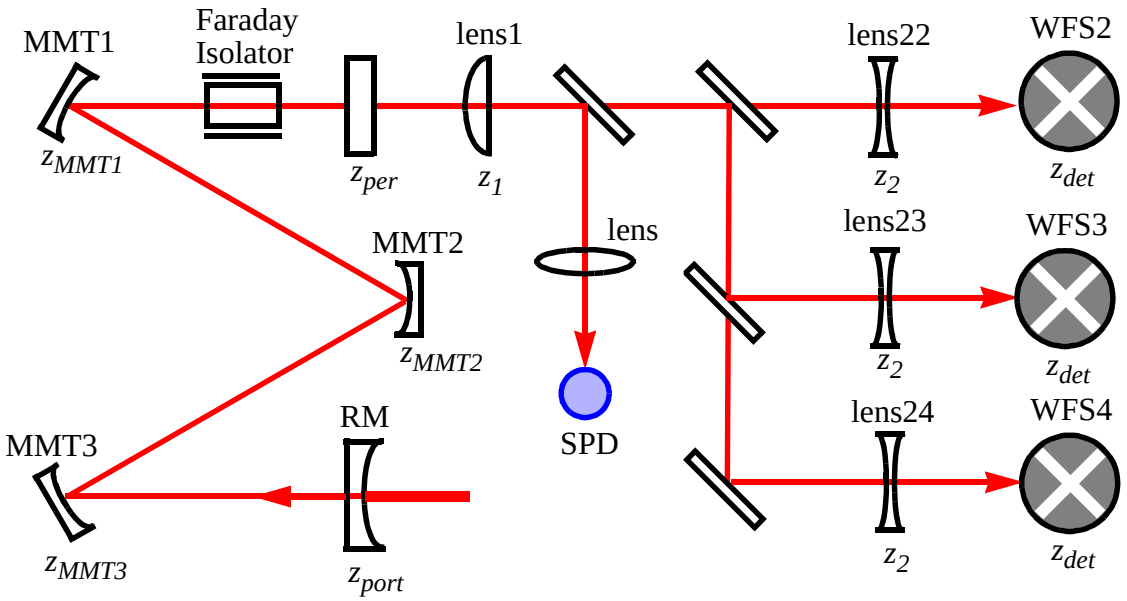

Figure 4: Schematic layout of the wavefront sensors at the reflection port. z_{port} is the location of the recycling mirror, which is also the reflection port. From the RM, the beam travels through the mode matching telescope (MMT), the Faraday isolator and arrives at the periscope on ISCT 1. We set $z = 0$ at the position of the beam waist of the beam returning from the MMT. z_{port} is the position of the RM; z_{MMTi} are the positions of the i-th MMT mirrors; z_{per} is the position of the periscope; z_1 is the position of the first lens, with focal length, f_1; z_2 is the position of the second lens, with focal length, f_2; and z_{det} is the position of the detector.

mirror passes through a mode matching telescope (MMT) [3], which alters its beam parameters. For the purposes of the design, we propagate the arm cavity beam through the mode matching telescope to determine the plane at which the MMT output beam has a waist. The waist position and size and the total Guoy phase accumulated from the interferometer beam waist to this plane are the inputs to the Guoy phase telescope optimization algorithm. Some parameters that are relevant to the calculation are listed in Table 4. The beam propagated through the reflection port MMT has an effective beam waist $w_0 = 1.739$ mm occurring 0.8702 m in front of (i.e. away from the vacuum viewport) the periscope. The total Guoy phase shift accumulated up to the periscope output is 346°.

Optical train	Geometric parameters	Relative position[a] (m)
Arm cavity beam waist	$w_0 = 3.13$ cm	0
ITM	$R = 14200$ m $\Rightarrow f = -31556$ m	613.6
RM	$R = 14900$ m $\Rightarrow f = -33111$ m	12.72
MMT3	$R = 25.16$ m $\Rightarrow f = 12.58$ m	17.218
MMT2	$R = 2.10$ m $\Rightarrow f = 1.05$ m	13.7774
MMT1	$R = 11.28$ m $\Rightarrow f = 5.64$ m	13.3161
Faraday rotator	$f = 60$ m	1.5836
Vacuum viewport	flat	1.5048
Periscope bottom mirror	flat	0.453

Table 4: The geometric parameters and positions of the optical elements between the arm cavity beam waist and the periscope on the reflection port output table for the 2 km configuration.

a. Position of the optical element relative to the previous element in the optical train, i.e. the spacing between adjacent optical elements.

The focal lengths and positions of the lenses and the position of the detector head for the reflection port telescopes is given in Table 5.

WFS (Φ_{Guoy})	Ifo	f_1	z_1	f_2	z_2	z_{det}	Δz
WFS 2 (145°)	4k	+1016.7	330.0	–76.3	1566.0	1988.9	-249.0
WFS 3 (0°)	4k	+1016.7	330.0	–76.3	1695.1	1967.1	-376.9
WFS 4 (90°)	4k	+1016.7	330.0	–76.3	1288.6	2345.4	28.4
WFS 2 (145°)	2k	+1016.7	330.0	–76.3	1371.5	2120.2	–120.7
WFS 3 (0°)	2k	+1016.7	330.0	–76.3	927.4	1220.0	323.4
WFS 4 (90°)	2k	+1016.7	330.0	–76.3	1293.9	2374.4	14.1

Table 5: The Guoy phase telescopes for the reflection port wavefront sensors for the 4 km and 2 km configurations. All distances are in mm and are specified from $z = 0$ at the location of the bottom mirror of the periscope on ISCT1.

The Gaussian beam propagation, along with Guoy phase shift along the telescope train is given in Figure 5 for the 2 km configuration.

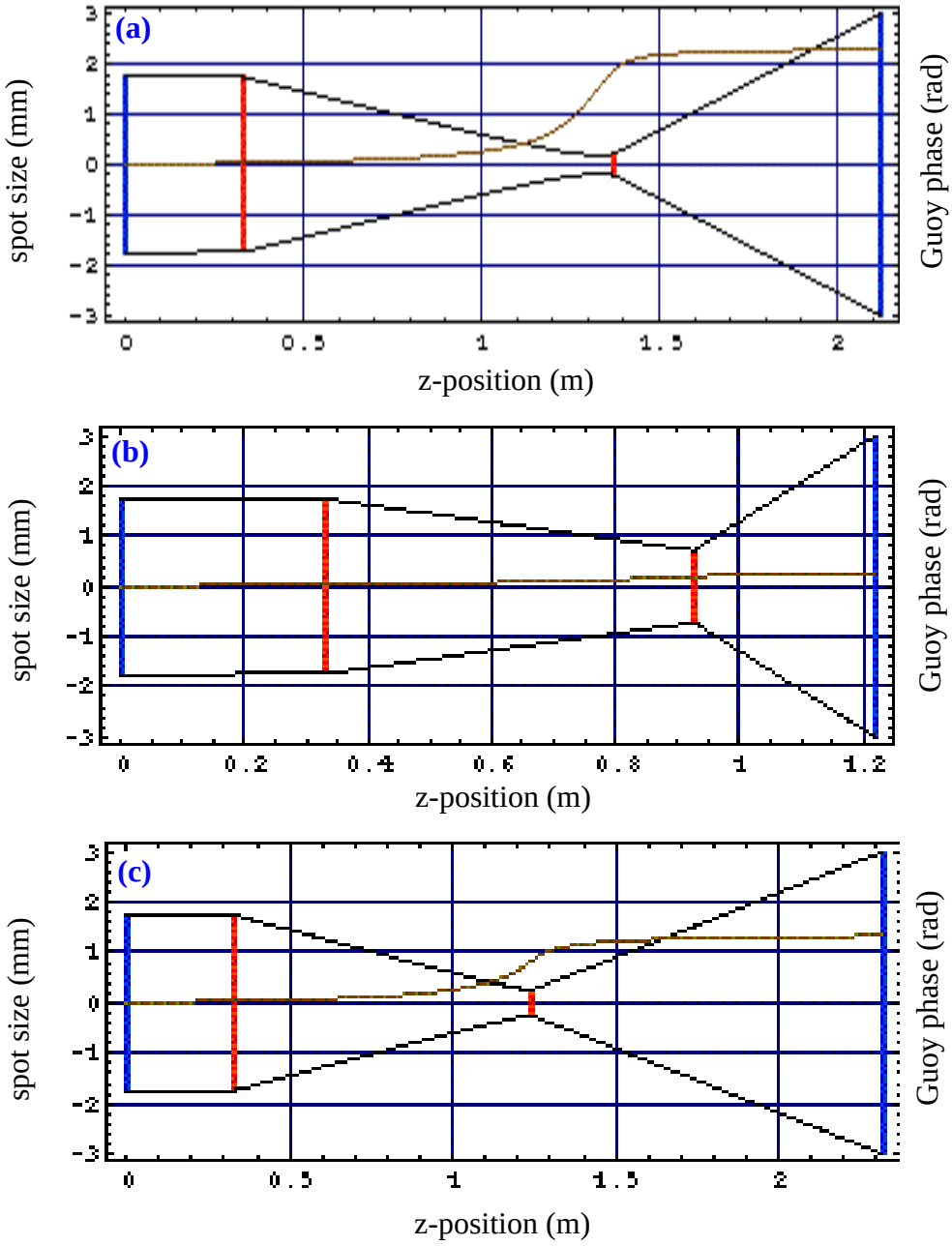

Figure 5: Gaussian beam profiles for the 2 km configuration for the reflection port sensors: (a) WFS 2, (b) WFS 3 and (c) WFS 4. The Guoy phase shifts are shown as the gold curves and do not include the 346° already accumulated by propagation from the interferometer beam waist out to the periscope output (z = 0 in the above plots).

While the 90° and 145° telescopes are fairly straightforward, the 0° (180°) telescopes can sometimes be pathological. By the time the beam has propagated to the periscope, it has acquired nearly 360° of Guoy phase shift. To acquire 180° of phase shift from a telescope with only one converging lens would require sampling the beam at nearly infinity.

Error propagation

i Antisymmetric port

The dominant source of Guoy phase error in the two-lens design is error in the position of the second lens. In fact, an error of ±10 mm in the placement of the second lens corresponds to a Guoy phase error of ±23° for WFS 1 at 90°. This error depends primarily on the focal length of the first (converging) lens. To reduce this error we would need to use a longer focal length which makes the Guoy phase telescope too long. The focal length of the second (diverging) lens is chosen to be as short as possible to keep the distance between the second lens and the detector head short. The infinity adjustment will be particularly useful for this telescope since it requires just 6 mm of space and will provide an accurate measure of the lens spacing. All other errors contribute less than ±0.5° to the Guoy phase error and less than ±0.2 mm to the spot size on the detector.

ii Reflection port

Again, the dominant source of Guoy phase error in the is error in the position of the second lens. An error of ±10 mm in the placement of the second lens corresponds to a Guoy phase error of ±5° for the detectors at 90°, a Guoy phase error of ±3° for the detectors at 145°, and a guoy phase error of less than ±1° for the 4k detector at 0°. All other errors contribute less than ±0.5° to the Guoy phase error and less than ±0.2 mm to the spot size on the detector.

References

[1] LIGO-T960113-00-DModal Model Update 1: Interferometer Operators (June 1996).

[2] LIGO-T960115-00-DModal Model Update 3: Small Angle Regime (Dec. 1996).

[3] LIGO-T980009-00-DInput Optics Final Design, pp. 56 – 62 (March 1998).

[4] LIGO-T960111-A -DWavefront Sensor (July 1996).

[5] LIGO-E980061-00-DCore Optics Final Design, p. 14 (April 1998).

[6] LIGO-T980009-00-DInput Optics Final Design, p. 36 (March 1998).

[7] LIGO-T980104-00-DCore Optics Support Final Design, p. 7 (November 1998).

[8] Mike Smith, PO_beam_path_length.xls (rev. January 18, 1999).

[9] LIGO-P970013-00-RAlignment Issues in Laser Interferometric Gravitational-wave Detectors, p. 71 (January 1997).

Appendix: Mode matching telescope and interferometer parameters

The parameters which are needed for the Guoy phase telescope design are listed in Table 6. The core optics radii of curvature are from [5]; recycling cavity lengths are inferred from the modulation frequencies listed in [6]; mode matching telescope parameters are from [3].

Parameter	Description	4k	2k
Rad_{ETM}	ETM radius of curvature	7400	7400
Rad_{ITM}	ITM radius of curvature	14200	14200
Rad_{RM}	RM radius of curvature	14900	14900
L_{arm}	nominal arm cavity length	4000	2000
l_{RC}	nom. recycling cav. length	9.2	12.72
$w0_{IFO}$	interferometer waist size	0.0351	0.0313
$zw0_{IFO}$	position of $w0_{IFO}$ from ITM (between ITM and ETM)	1000	614
Rad_{BRT1} (APS)	BRT1 radius of curvature		
Rad_{BRT2} (APS)	BRT2 radius of curvature		
Rad_{BRT1} (PO)	BRT1 radius of curvature		
Rad_{BRT2} (PO)	BRT2 radius of curvature		
Rad_{MMT1}	MMT1 radius of curvature	6.76	11.28
Rad_{MMT2}	MMT2 radius of curvature	3.16	2.10
Rad_{MMT3}	MMT3 radius of curvature	25.16	25.16

Table 6: Interferometer and mode matching telescope parameters for the 4k and 2k configurations. All quantities listed are in meters.

There are small discrepancies between the interferometer parameters listed in Table 27 in Ref. [3] that need to be sorted out. Small adjustments of the Guoy phase telescope design will be made accordingly.